

Local polariton modes and resonant tunneling of electromagnetic waves through periodic Bragg multiple quantum well structures

Lev I. Deych[†], Alexey Yamilov[‡], and Alexander A. Lisyansky[‡]

[†] Department of Physics, Seton Hall University, South Orange, NJ 07079

[‡] Department of Physics, Queens College of CUNY, Flushing, NY

(December 2, 2024)

We study analytically defect polariton states in Bragg multiple-quantum-well structures and defect induced changes in transmission and reflection spectra. Defect layers can differ from the host layers in three ways: exciton-light coupling strength, exciton resonance frequency, and inter-well spacing. We show that a single defect leads to two local polariton modes in the photonic bandgap. These modes cause peculiarities in reflection and transmission spectra. Each type of defect can be reproduced experimentally, and we show that each of these plays a distinct role in the optical properties of the system. For some defects, we predict a narrow transmission window in the forbidden gap at the frequency set by parameters of the defect. We obtain analytical expressions for corresponding local frequencies as well as for reflection and transmission coefficients. We show that the presence of the defects leads to resonant tunneling of the electromagnetic waves via local polariton modes accompanied by resonant enhancement of the field inside the sample, even when a realistic absorption is taken into account. On the basis of the results obtained, we make recommendations regarding the experimental observation of the effects studied in readily available samples.

I. INTRODUCTION

Optical properties of multiple quantum wells (MQW) have attracted a great deal of interest recently^{1–8}. Unlike other types of superlattices, excitons in MQW are confined in the planes of the respective wells, which are separated by relatively thick barriers. Therefore, the only coupling between different wells is provided by the radiative optical field. The coupling results in MQW polaritons – coherently coupled quasi-stationary excitations of quantum well (QW) excitons and transverse electromagnetic field. The spectrum of short MQW structures consists of a number of quasi-stationary (radiative) modes with finite life-times. This spectrum is conveniently described in terms of super- or sub-radiant modes^{1,3,4}. When the number of wells in the structure grows, the life-time of the former decreases, and the life-time of the latter increases. In longer MQW, however, this approach becomes misleading, as discussed in Ref. 9, and a more appropriate description is obtained in terms of stationary modes of an infinite periodic structure. The spectrum of MQW polaritons in this case consists of two branches separated by a gap with a width proportional to the exciton-light coupling constant Γ ^{1,3}. In a number of papers^{2,5,7,8} it was shown that the width of the polariton bandgap can be significantly increased by tuning the interwell spacing, a , to the Bragg condition, $a = \lambda_0/2$, where λ_0 is the wavelength of the light at the exciton frequency Ω_0 . Under this condition, boundaries of two adjacent gaps become degenerate, and one wider gap with the width proportional to $\sqrt{\Gamma}$ is formed. Detuning of the lattice constant from the exact Bragg condition removes the degeneracy and gives rise to a conduction band in the center of the Bragg gap⁹. A well-pronounced Bragg polariton gap was observed in recent experiments⁸ with *GaInAs/GaAs* Bragg structures with the number of wells up to 100. These experiments convincingly demonstrate that despite homogeneous and inhomogeneous broadening, the coherent exciton-photon coupling in long MQW is experimentally feasible. Polariton effects arising as a result of this coupling open up new opportunities for manipulating optical properties of quantum heterostructures.

One such opportunity is associated with introducing defects in MQW structures. These defects can be either QW's of different compositions replacing one or several "host" wells, or locally altered spacing between elements of the structure. It is well known in the physics of regular crystals (see, for instance, Ref. 10) that local violations of otherwise periodic structures can lead to the appearance of local modes with frequencies within spectral gaps of host structures. This idea was first applied to MQW in Ref. 11, where it was shown that different defects can indeed give rise to local exciton-polariton modes in infinite MQW. Unlike regular local modes in 3-*d* periodic structures, these modes are localized only in the growth direction of the MQW, while they can propagate along the planes of the wells. Therefore, one should clearly distinguish these defect polariton modes from well known interface modes in layered systems or non-radiative two-dimensional polariton modes in ideal MQW.^{12–14} The latter exist only with the in-plane

wave numbers, $k_{||}$, exceeding certain critical values, while the local mode in a defect MQW structure exists at $k_{||} = 0$ and can be excited even at normal incidence.

In this paper we present results of detailed studies of local polariton modes (LPM's) produced by four different types of individual defects in Bragg MQW structures. The peculiar structure of Bragg MQW's results in a wider than usual polariton gap, which is actually formed by two gaps with degenerate boundaries. This property has a profound effect on the properties of local modes, leading, for instance, to emergence of two local states from a single defect. In this paper we neglect in-plane disorder in individual QW's, and assume that apart from a deliberately introduced single defect, the structure remains ideally periodic. We consider LPM's with zero in-plane wave vector only. Such modes can be excited by light incident in the growth direction of the structure, and can result in resonance transmission of light with gap frequencies. This effect is studied both analytically and numerically with homogeneous broadening taken into account phenomenologically. Equations describing dynamics of the light-exciton interaction in this situation are essentially equivalent to a model of the one-dimensional chain of dipoles used in the series of our previous works where LPM's in polar crystals were discussed.^{15–17} Similar equations also appear in the theory of atomic optical lattices.¹⁸ The essential difference between results presented in this paper and previous studies stems from the peculiarities of the Bragg arrangement. Using Greens' function and transfer matrix formalisms, we study both eigen frequencies of LPM's for different types of defects and transmission properties of the defect structures. Taking into account homogeneous broadening and using parameters of the system studied experimentally in Ref. 8, we predict which defects will produce the most significant changes in transmission and reflection properties of realistic MQW structures.

II. DEFECT MODES IN BRAGG MQW

In order to describe optical properties of QW's one has to take into account the coupling between retarded electromagnetic waves and excitons. This is usually done with the use of the non-local susceptibility determined by energies and wave functions of a QW exciton^{1,14}. The treatment of the exciton subsystem can be significantly simplified if the interwell spacing is much larger than the size of a well itself. In *InGaAs/GaAs* MQW structures studied in Ref. 8, on which we base our numerical examples, the width of the QW layer amounts only to about 10% of the period of the structure. In this case, one can neglect the overlap of the exciton wave functions from neighboring wells and assume that an interaction between well excitons occurs only due to coupling to the light. It is also important that the width of the wells is considerably smaller than the exciton's Bohr radius, and therefore one can neglect the spatial extent of the wells, and describe them with a polarization density of the form: $\mathbf{P}(\mathbf{r}, z) = \mathbf{P}_n(\mathbf{r})\delta(z - z_n)$, where \mathbf{r} is an in-plane position vector, z_n represents a coordinate of the n -th well, and \mathbf{P}_n is a surface polarization density of the respective well. The latter is determined by the exciton dynamics, described in the considered situation by the equations

$$(\Omega_n^2 - \omega^2) P_n = \frac{1}{\pi} c \Gamma_n E(z_n), \quad (1)$$

$$\frac{\omega^2}{c^2} E(z) + \frac{d^2 E(z)}{dz^2} = -4\pi \frac{\omega^2}{c^2} \sum_n P_n \delta(z - z_n), \quad (2)$$

where Ω_n and Γ_n are exciton frequency and exciton-light coupling of the n -th QW, respectively. In an infinite pure system, all $\Gamma_n = \Gamma_0$, $\Omega_n = \Omega_0$, $z_n = na$, where $a = \lambda_0/2$ is the Bragg's interwell separation. Eq. (2) describes an electromagnetic wave of one of the degenerate transverse polarizations, propagating in the growth direction of the structure. This equation coincides with equations used in Refs. 15–18 for one-dimensional chains of atoms.

The spectrum of ideal periodic MQW's has been studied in many papers.^{1,3,9,18–20} In the specific case of Bragg structures, the exciton resonance frequency, Ω_0 , is at the center of the bandgap determined by the inequality $\omega_l < \omega < \omega_u$, where $\omega_l = \Omega_0 \left(1 - \sqrt{2\Gamma_0/\pi\Omega_0}\right)$ and $\omega_u = \Omega_0 \left(1 + \sqrt{2\Gamma_0/\pi\Omega_0}\right)$.⁹ This bandgap is the frequency region where we will look for new local states associated with the defects. In this paper, we consider four types of such defects. First of all, one can replace an original QW with a QW with different exciton frequency (Ω -defect). This can be experimentally achieved by varying the composition of the semiconductor in the well. Another possibility is to change the coupling constant (Γ -defect) at one of the wells. Again, experimental realization of this defect is rather straightforward, one can simply change the width of the QW layer. Indeed, since the width of the well is assumed to be small comparing to the interwell spacing, one can neglect the shift of the positions of the rest of the wells. The third possibility is to perturb an interwell spacing between two wells. Here we will distinguish two defects: a - and b -defects. In the first one, the interwell spacing is changed (Fig. 1a). It can be seen that this induces a shift in position of all the wells that follow the defect, making it significantly nonlocal in contrast with the b -defect, when one

shifts one well keeping positions of the rest unchanged (Fig. 1b). Experimental realizations of these two defects is simple and can be done at the sample growth stage. In the following section we show that each of these types affects the optical properties of the MQW lattice in remarkably different ways.

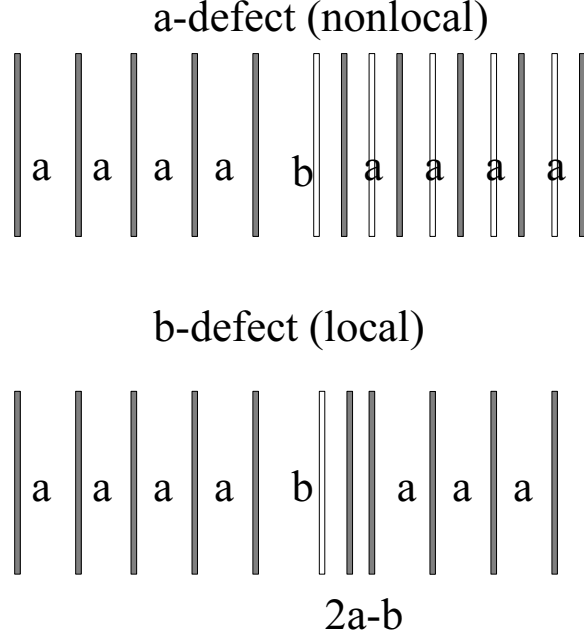


FIG. 1. Two types of interwell spacing defects. The nonlocal a-defect (a) as opposed to the local b-defect (b). Solid bars represent locations of QW's in the defect lattice. The empty bars represent what would have been a perfectly ordered MQW lattice.

We start with Ω - and Γ -defects which are similar in a sense that they both introduce perturbations in the equation of motion, Eq. (1), that are localized at one site (the diagonal disorder). Therefore, they can be studied by the usual Green's function technique like the one used to treat the localized phonon states in impure crystals (see, for instance, Ref. 10). Using the Green's function, the polarization of the n -th QW can be expressed in terms of the polarization on the defect QW, P_{n_0} as

$$P_n = G(n - n_0)P_{n_0}.$$

Allowing $n = n_0$, one obtains the equation for an eigenfrequency of LPM:

$$F_{\Omega,\Gamma} = \frac{2\Gamma_0\omega \sin(k_0a) / (\omega^2 - \Omega_0^2)}{\sqrt{[\cos(k_0a) + 2\Gamma_0\omega \sin(k_0a) / (\omega^2 - \Omega_0^2)]^2 - 1}}, \quad (3)$$

where $k_0 = \omega/c$ and the function $F_\Omega = (\omega^2 - \Omega_0^2) / (\omega^2 - \Omega_0^2)$ for the Ω -defect and the respective function is $F_\Gamma = \Gamma_0 / (\Gamma_1 - \Gamma_0)$ for the Γ -defect, Ω_1 and Γ_1 denote respective parameters of the defect layer. A similar equation for the Ω -defect has been studied in Ref. 15 in the longwave approximation. It was found that the equation has one real valued solution for any $\Omega_1 > \Omega_0$. In the case of the Bragg structures, there are always two solutions for both types of defects, one below Ω_0 and one above. This is a manifestation of the fact that the bandgap consists of two gaps positioned one right after the other. The above equations can be solved approximately when $\Gamma_0 \ll \Omega_0$, which is the case for most materials. For the Ω -defect, one solution demonstrates a radiative shift from the defect frequency Ω_1 ,

$$\omega_{def}^{(1)} = \Omega_1 - \Gamma_0 \frac{\Omega_1 - \Omega_0}{\sqrt{(\omega_u - \Omega_1)(\Omega_1 - \omega_l)}}, \quad (4)$$

while the second solution splits off the upper or lower boundary depending upon the sign of $\Omega_1 - \Omega_0$:

$$\omega_{def}^{(2)} = \omega_{u,l} \pm \frac{1}{2}(\omega_u - \omega_l) \left(\frac{\pi}{2} \frac{\Omega_1 - \Omega_0}{\Omega_0} \right)^2, \quad (5)$$

where one chooses ω_u and “–” for $\Omega_1 < \Omega_0$, and ω_l and “+” in the opposite case. This is illustrated in Fig. 2a. It can be seen that the shift of $\omega_{def}^{(1)}$ from the defect exciton frequency Ω_1 is negative for $\Omega_1 > \Omega_0$ and positive for $\Omega_1 < \Omega_0$. The magnitude of the shift is of the order of the coupling constant Γ_0 , which is usually rather small, and this fact, as it is shown in the next section, is crucial for the optical properties of the defect. The second local mode $\omega_{def}^{(2)}$ lies very close to the edges of the bandgap, and it would be, therefore, very difficult to distinguish from the modes making up the allowed bands even for negligible dissipation.

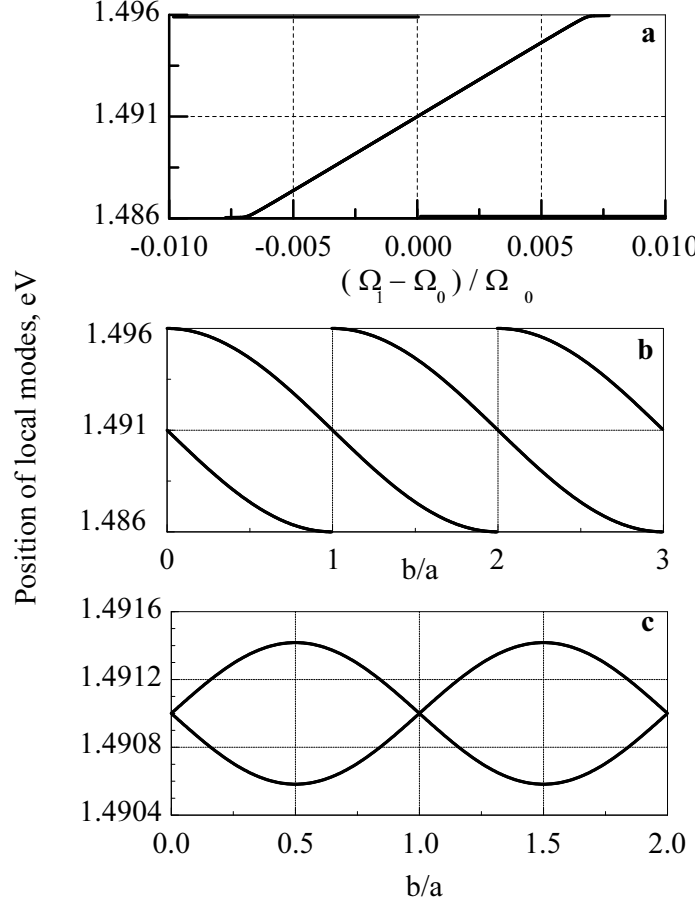


FIG. 2. Positions of the local modes in the bandgap (1.486 - 1.496 eV) for the Ω -defect (a), a -defect (b), and b -defect (c) as functions of the defect strengths.

In the case of the Γ -defect, one again finds two solutions of Eq. (3):

$$\omega_{def}^{(1,2)} = \omega_{u,l} \pm 2(\Gamma_1 - \Gamma_0)^2 (\omega_u - \omega_l). \quad (6)$$

which exist only for $0 < \Gamma_1 < \Gamma_0$ and are very close to the gap boundaries. The situation is similar to the second solution for the Ω -defect, and one can conclude, therefore, that the Γ -defect would not affect significantly the optical spectra of the system.

The next defect we consider, the a -defect, is shown in Fig. 1a. One can see that this defect differs from the other two in a fundamental way. An increase in an interwell distance between any two wells automatically changes the coordinates of an infinite number of wells: $z_n = na$ for $n \leq n_d$ and $z_n = (b - a) + na$ for $n_d < n$, where b is the distance between the n -th and $(n + 1)$ -th wells. Therefore, this defect is non-local and cannot be solved by the same methods as the two previous cases. The best approach to this situation is to match solutions of semi-infinite chains for $n < n_d$ and $n > n_d + 1$ with a solution for $na < z < na + (b - a)$, which is schematically shown in Fig. 3. Solutions for semi-infinite chains can be constructed using the transfer matrix approach. The state of the system at the m -th well is described by a two dimensional vector v_m with components $E(x_m)$ and $(1/k_0)(dE(x_m)/dx)$:

$$v_m = \prod_{n=1}^m \hat{\tau}_n v_0 = \hat{T} v_0. \quad (7)$$

The 2×2 transfer matrix $\hat{\tau}_n$ at the n -th well is

$$\hat{\tau}_n = \begin{pmatrix} \cos(k_0 a_n) + \beta \sin(k_0 a_n) & \sin(k_0 a_n) \\ -\sin(k_0 a_n) + \beta \cos(k_0 a_n) & \cos(k_0 a_n) \end{pmatrix}, \quad (8)$$

where $a_n = x_{n+1} - x_n$ and $\beta = 4\Gamma_0 \omega / (\omega^2 - \Omega_0^2)$ is the polarizability of the well. The eigen states for a finite system, $n \in (1, N)$, can be found if one looks for non-trivial solutions when no incident wave is present in the system. This corresponds to the boundary conditions of the form

$$v_0 = \begin{pmatrix} r \\ -ir \end{pmatrix} \text{ and } v_N = \begin{pmatrix} t \\ it \end{pmatrix}.$$

A resulting dispersion equation for the eigen frequencies can be expressed in terms of the elements of the total transfer matrix \hat{T} :

$$(T_{11} + T_{22}) - i(T_{12} - T_{21}) = 0. \quad (9)$$

It is clear that for finite samples the solutions of this equation are complex, reflecting the fact that the modes are not stationary; they have lifetimes which tend to infinity only in the limit $N \rightarrow \infty$.

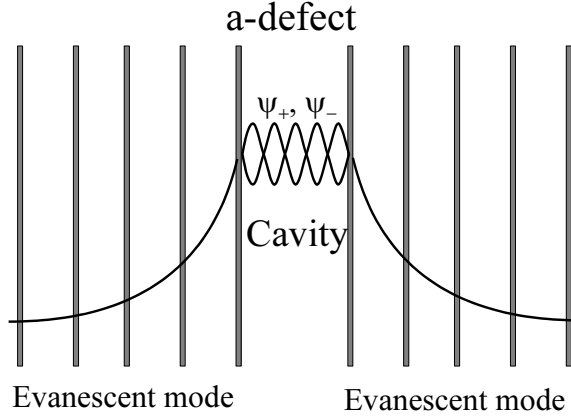


FIG. 3. Matching the solutions for half-infinite perfect MQW with cavity modes ψ_{\pm} one can obtain the dispersion equation for (quasi)local modes (in finite systems) of such a system with the defect.

Eq. (9) for the a -defect in the infinite MQW system, after some cumbersome but straightforward algebra, can be presented in the form

$$\cot(k_0 b) = -\frac{\sin(k_0 a) - \beta \lambda_- / 2}{\cos(k_0 a) - \lambda_-}, \quad (10)$$

where $\lambda_- = [\cot(k_0 a) + \beta/2 - \sqrt{D}] \sin(k_0 a)$ is one of the eigenvalues of the transfer matrix, Eq. (8), and $D = -1 + \beta^2/4 + \beta \cot(k_0 a)$. This equation, as well as in the cases of Γ - and Ω -defects, has two solutions - above and below Ω_0 . These solutions can be approximated as

$$\omega_{def}^{(1)} = \Omega_0 - \frac{\omega_u - \omega_l}{2} \frac{(-1)^{[\frac{\xi+1}{2}]} \sin(\pi \xi / 2)}{1 + \frac{\omega_u - \omega_l}{2\Omega_0} \xi (-1)^{[\frac{\xi+1}{2}]} \cos(\pi \xi / 2)}, \quad (11)$$

$$\omega_{def}^{(2)} = \Omega_0 + \frac{\omega_u - \omega_l}{2} \frac{(-1)^{[\frac{\xi+1}{2}]} \cos(\pi \xi / 2)}{1 - \frac{\omega_u - \omega_l}{2\Omega_0} \xi (-1)^{[\frac{\xi+1}{2}]} \sin(\pi \xi / 2)}, \quad (12)$$

where $\xi = b/a$, and [...] denotes an integer part. Therefore, for $\Gamma_0 \ll \Omega_0$ and not very large ξ , $\xi \ll (\Omega_0/\Gamma_0)^{1/2} \simeq 10^2$, and both solutions are almost periodic functions of b/a with the period of 1, as shown in Fig. 2b. These solutions oscillate between respective boundaries of the gap (ω_u or ω_l) and the exciton frequency Ω_0 . At the integer values of ξ , one of the frequencies $\omega_{def}^{(1)}$ or $\omega_{def}^{(2)}$ becomes equal to Ω_0 , and the other reaches ω_u or ω_l depending upon the parity of ξ . When ξ crosses an integer value, the solution passing through Ω_0 changes continuously, while the second one experiences a jump toward the opposite gap boundary. The observable manifestations of the defect modes (for instance, transmission resonances as described in the next section of this paper) vanish when the defect frequencies approach the gap boundaries. This jump, therefore, would manifest itself as a disappearance of the transmission peak near one of the gap boundaries, and a gradual reappearance at the opposite edge as ξ changes through an integer value. It is interesting to note again that the exciton resonance frequency Ω_0 , which formally lies at the center of the gap, behaves as one of the gap boundaries. This is another manifestation of the fact that the polariton gap in the Bragg structures is formed by two adjacent gaps with a degenerate boundary at Ω_0 .

Calculations of the defect frequencies for the b -defect can be done in the framework of both schemes. The transfer-matrix approach, however, turns out to be less cumbersome. The dispersion equation for LPM's in this case takes the form

$$0 = \frac{\beta^2}{2} \sin^2(k_0(b-a)) \left[-1 + \frac{\beta}{2\sqrt{D}} + \frac{\cot(k_0a)}{2\sqrt{D}} \right] + \cos^2(k_0a) + \sin^2(k_0a) \left(\frac{\beta}{2} - \sqrt{D} \right)^2 + \sin(2k_0a) \left(\frac{\beta}{2} - \sqrt{D} \right). \quad (13)$$

This equation can be solved approximately assuming that the splitting of the solution from the Bragg frequency, Ω_0 , is much smaller than the width of the gap. Expanding different terms of Eq. (13) in terms of powers of $(\omega - \Omega_0)$ and keeping the lowest non-zero contribution, one obtains two different solutions for frequencies of LPM's:

$$\omega_{def}^{(1,2)} = \Omega_0 \left[1 \pm \left(\frac{2}{\pi} \right)^{1/4} \left(\frac{\Gamma_0}{\Omega_0} \right)^{3/4} |\sin \pi(\xi - 1)| \right]. \quad (14)$$

The splitting of these modes from Ω_0 is of the order of $(\Gamma_0/\Omega_0)^{3/4}$, and is much smaller than the width of the gap, which is proportional to $(\Gamma_0/\Omega_0)^{1/2}$ in accord with our initial assumption. Similar to the case of a -defect, these frequencies change periodically with ξ , but unlike the previous case, they both split off the center of the gap, Ω_0 , and at integer values of ξ merge back to Ω_0 . The maximum deviations of the local frequencies from Ω_0 are of the order of $(\Gamma/\Omega_0)^{3/4}$ and take place for half-integer values of ξ .

One can notice that the b -defect involves two adjacent wells, and in the Green's function approach one would have to deal with a system of two coupled equations. Accordingly, it can be expected that there must be four possible local frequencies (two in each half of the gap), while we found only two of them. The reason for this is that the Bragg condition makes a pair of frequencies, which are both above or below Ω_0 , nearly degenerate, and the difference between them is much smaller than the terms we kept in our approximate solution. This can be understood if one notices that the transfer matrices in Eq. (8) contain factors $\cos(kb)$, $\sin(kb)$ and $\cos[k(2a-b)]$, $\sin[k(2a-b)]$ for the first and the second of the involved wells, respectively. Exactly at the Bragg frequency, $ka = \pi$, these factors coincide leading to the degeneracy. Since the shift of the actual local frequency from the Bragg frequency is relatively small, the solutions remain nearly degenerate. The fact that obtained solutions are symmetrical with respect to the replacement of b with $2a - b$ is not surprising and reflects the symmetry of the transfer matrices discussed above.

III. DEFECT LPM'S AND TRANSMITTANCE AND REFLECTANCE EXPERIMENTS

In this Section we study how the local defect modes obtained above affect the reflection and transmission spectra of the finite size periodic Bragg MQW's in the presence of homogeneous broadening.

Transmission and reflection coefficients can be expressed in terms of the elements of the total transfer matrix defined by Eq. (7) as

$$T = |t|^2 = \left| \frac{2 \det \hat{T}}{(T_{11} + T_{22}) - i(T_{12} - T_{21})} \right|^2, \quad (15)$$

$$R = |r|^2 = \left| -\frac{(T_{11} - T_{22}) + i(T_{12} + T_{21})}{(T_{11} + T_{22}) - i(T_{12} - T_{21})} \right|^2. \quad (16)$$

Without absorption, T and R in the form of Eqs. (15) and (16) can be shown to add up to unity. In the denominators of T and R one can recognize the dispersion relation Eq. (9) that was obtained in the previous section by matching the decaying solutions on both sides of the defect.

Γ - and Ω -defects differ from the original QW's only by the polarizability β , therefore, they both can be dealt with at the same time if one introduces the defect parameter $\varepsilon = (\beta_{def} - \beta) / 2\sqrt{D}$, which is equal to zero when $\beta_{def} = \beta$. The exact expression for T is cumbersome, however, for the systems longer than the localization length one can neglect by smaller eigenvalue of the total transfer matrix, which is proportional to $\exp(-Na/l_{loc}(\omega))$. In this case, the expression for the transmission coefficient can be simplified to¹⁵

$$t = \frac{t_0}{(1 + \varepsilon) + i \exp(-ik_0 Na) \varepsilon \Phi t_0 \cosh[(N - 2n_0 + 1)\kappa a]}. \quad (17)$$

Here n_0 is the position of the defect QW, $\kappa = 1/l_{loc}(\omega)$, and $\Phi = \beta/(\sin(k_0 a) \sqrt{D})$. For $\varepsilon = 0$, Eq. (17) gives the transmission coefficient, t_0 , of the pure system,

$$t_0 = \frac{2e^{ikL} \exp(-\kappa L)}{1 + i[2 - \beta \cot(ka)]/\sqrt{D}}, \quad (18)$$

exhibiting an exponential decay characteristic of the evanescent modes from a band gap.

Eq. (17) describes the resonance tunneling of the electromagnetic waves through MQW with the defect. The equation

$$1 + \varepsilon = 0$$

can be shown to coincide with the dispersion equations for local defect modes of the infinite structure in the case of Ω and Γ defects. Given this fact and the structure of Eq.(17), it seems natural to assume, as we did in our previous papers¹⁵ that the transmission reaches its maximum value at the frequencies of the local modes. More careful consideration showed, however, that the systems under consideration behave in a less trivial way, and that maxima of the transmission occur at frequencies shifted from the frequency of the local modes. This is a quite unusual behavior that distinguish the systems under consideration from other instances of resonance tunneling. Moreover, we shall show that contrary to our previous result¹⁵, transmission at the maximum is always equal to unity (in the absence of absorption).

Numerical calculations showed that the distinctive resonance transmission occurs only if local modes lie not too close to the boundaries or the center (which is, strictly speaking, also a degenerate boundary) of the gap. Γ defects, therefore, can be excluded from consideration, as well as one of the solutions for the Ω -defect. For frequencies close to the remaining local mode (the solution for the Ω -defect given by Eq. (4)) the expression for the transmission coefficient Eq. (17) can be simplified. Expansion in the vicinity of the local mode gives

$$T = \frac{\left(\frac{\omega - \Omega_1}{\omega_{def} - \Omega_1}\right)^2}{1 + A_1 \left| \frac{\omega - \omega_T \cosh((N - 2n_0 + 1)\kappa a) (1 + i \cdot A_2)}{\omega_{def} - \omega_T} \right|^2 \cdot \left(\frac{\omega_T - \Omega_1}{\omega_{def} - \Omega_1}\right)^2}, \quad (19)$$

Parameters A_1 , A_2 and ω_T are defined by

$$A_1 = \frac{(\omega_+ - \omega_{def})^2 (\omega_{def} - \omega_-)^2}{4(\omega_{def} - \Omega_0)^2 (\omega_{def} - \omega_l) (\omega_u - \omega_{def})}, \quad (20)$$

$$A_2 = \frac{(\omega_{def} - \Omega_0) \sqrt{(\omega_{def} - \omega_l)(\omega_u - \omega_{def})}}{(\omega_+ - \omega_{def})(\omega_{def} - \omega_-)} \tanh[(N - 2n_0 + 1)\kappa a], \quad (21)$$

$$\omega_T = \omega_{def} + \pi \frac{(\omega_+ - \omega_{def})(\omega_{def} - \omega_-)}{\Omega_0} \frac{(\omega_{def} - \Omega_0)}{\sqrt{(\omega_{def} - \omega_l)(\omega_u - \omega_{def})}} e^{-\kappa Na} \quad (22)$$

where $\omega_{\pm} = \Omega_0 \pm (\omega_u - \Omega_0) / \sqrt{2}$. Resonance transmission occurs when the defect layer is located in the center of the system $N - 2n_0 + 1 = 0$. In this case the coefficient A_2 becomes zero and Eq. (19) can be presented in the following form

$$T = \frac{4\gamma_\Omega^2}{Q^2} \frac{(\omega - \omega_T + Q)^2}{(\omega - \omega_T)^2 + 4\gamma_\Omega^2}, \quad (23)$$

where $Q = \omega_T - \Omega_1$, and the parameter γ_Ω is given by

$$\gamma_\Omega = \pi\Omega_0 \left(\frac{\omega_{def} - \Omega_0}{\Omega_0} \right)^2 e^{-\kappa Na}. \quad (24)$$

The transmission spectrum described by Eq.(23) has a shape known as a Fano resonance²¹, where ω_T is the resonance frequency, at which transmission turns to unity, and parameters γ_Ω and Q describe the width and the asymmetry of the resonance respectively. One can see from Eq.(22) that in general the transmission resonance frequency is shifted with respect to the frequency of the local mode. The shift, though exponentially small for long systems considered here, is of the same order of magnitude as the width of the resonance γ_Ω , and is, therefore, significant. These two frequencies, ω_T and ω_{def} , coincide in the special case when $\omega_{def} = \omega_\pm$. The fact that the transmission is equal to one, in this particular case, was obtained in our previous paper Ref. 15.

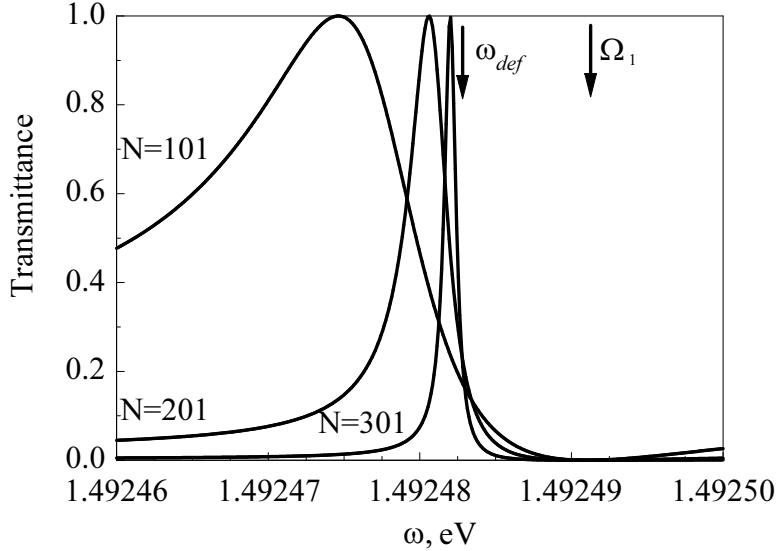


FIG. 4. The shape of the transmission maximum for 3 lengths $N = 101, 201, 301$. For all lengths, the Ω -defect is in the center of the system. $\Omega_1 = 1.492491$ eV.

At $\omega = \omega_T - Q = \Omega_1$ the transmission equals zero, which is a signature of Fano resonances. Usually the presence of Fano resonances is associated with interaction between a discrete level and a continuum of states; in the situation under consideration the role of the continuum is played by 2-d exciton states in the defect well. The shape of the Fano spectrum in an ideal system without absorption is determined by interplay between the width parameter γ_Ω and the asymmetry parameter Q . The former exponentially decreases with the increase of the length of the system, while the latter is length independent. However, the pre-exponential factor in γ_Ω is of the order of the exciton resonance frequency, Ω_0 , while Q is of the order of Γ , i.e. significantly smaller. Therefore, in principle, there are two possible cases: $\gamma_\Omega \gg Q$ for shorter systems ($1 \ll \kappa Na \ll \log(\Omega_0/Q)$), and $\gamma_\Omega \ll Q$ for longer systems. In the first case the transmission spectrum has a distinctively Fano-like asymmetrical shape, while in the second limit the spectrum attains a symmetrical Lorentzian shape characteristic for Wigner-Breight²² resonances. Fig. 4 shows the evolution of the shape of the transmission resonance in the absence of absorption from Fano-like to Wigner-Breight-like behavior with increase in the length of the system. One can also see from this figure how the position of the transmission maximum moves with the increase of the length. An actual possibility to observe the Fano resonance in the considered situation depends strongly upon the strength of absorption in the system, which must be at least smaller than Q . More detailed discussion of absorption related effects is given below in the present section.

Calculation of the transmission coefficient for the a -defect can be carried out in a similar manner. Dropping the exponentially small contribution from the smaller eigenvalue the transmission matrix can be written in the following form:

$$t = \frac{t_0}{(1 + \varepsilon_a) + ie^{-i\frac{\omega}{c}Na}\Phi^2 \sin(\frac{\omega}{c}(b-a))t_0 \cosh[(N - 2n_0)\kappa a]}, \quad (25)$$

where

$$\varepsilon_a = \frac{\sin\left(\frac{\omega}{c}b\right) - \sin\left(\frac{\omega}{c}a\right) - \lambda_+ \left(1 - \frac{\beta}{2\sqrt{D}}\right) \sin\left(\frac{\omega}{c}(b-a)\right)}{\sin\left(\frac{\omega}{c}a\right)}.$$

Similar to the previous defects, $1 + \varepsilon_a = 0$ coincides with the dispersion equation for an infinite system, but the transmission resonance is shifted with respect to the local mode. In the vicinity of the resonance Eq.(25) can be presented as:

$$T = \frac{1}{1 + A_1 \left| \frac{\omega - \omega_T \cosh((N-2n_0)\kappa a) (1 + i \cdot A_2)}{\omega_{def} - \omega_T} \right|^2}, \quad (26)$$

where parameters A_1 and A_2 are again given by Eq.(20) and Eq.(21) respectively. One only needs to replace $N-2n_0+1$ in Eq.(21) with $N-2n_0$, which reflects the new symmetry of the system. The frequencies of local modes ω_{def} are now given by Eqs. (11) and (12), and ω_T is defined by

$$\omega_T = \omega_{def} + 2(\omega_{def} - \Omega_0) \frac{(\omega_+ - \omega_{def})(\omega_{def} - \omega_-)(\omega_{def} - \omega_l)(\omega_u - \omega_{def})}{(\omega_u - \Omega_0)^4} e^{-\kappa Na}. \quad (27)$$

The resonance transmission again occurs when $N-2n_0 = 0$, which requires an even number of wells in the system. Eq.(26) in this case takes the standard Wigner-Breight shape

$$T = \frac{4\gamma_a^2}{(\omega - \omega_T)^2 + 4\gamma_a^2}, \quad (28)$$

with the half-width, γ_a , given now by

$$\gamma_a = 2 \frac{(\omega_{def} - \Omega_0)^2 (\omega_{def} - \omega_l)^{3/2} (\omega_u - \omega_{def})^{3/2}}{(\omega_u - \Omega_0)^4} e^{-\kappa Na}, \quad (29)$$

The frequency ω_T , where the transmission coefficient takes the maximum value of unity, is again shifted from the frequency of the defect mode. The two frequencies coincide, however, when the defect frequency is made equal to ω_{\pm} , which are the same frequencies at which transmission resonance and the local mode coincide for the Ω -defect. As one can see from Eq. (11), these conditions can be satisfied simultaneously for both defect frequencies of the a -defect when $b \simeq (\text{integer} + 1/2)a$ (see Fig. 2b). In this case the position of the transmission resonance becomes independent of the length of the system.

Finally, the b -defect gives an expression for the transmission coefficient very similar to Eq. (17) with the only distinction that ϵ has to be replaced by a different expression, which is too cumbersome to be displayed here. The maximum transmission for a given defect is again achieved when the defect is in the center of the system (N is odd). Expanding the transmission coefficient near the frequency of the respective local mode, one obtains

$$T = \frac{1}{1 + \frac{1}{4} \left(\frac{\omega_u - \Omega_0}{\omega_{def} - \Omega_0} \right)^2 \left| \frac{\omega - \omega_T}{\omega_{def} - \omega_T} + i \cdot \sinh((N-2n_0+1)\kappa a) \right|^2}, \quad (30)$$

with ω_T now given by

$$\omega_T = \omega_{def} - 2(\omega_{def} - \Omega_0) e^{-\kappa Na}. \quad (31)$$

Unlike other types of defects, in this case the transmission resonance is always different from ω_{def} . When the defect is at the resonance position $N-2n_0+1=0$, the transmission spectrum again takes the Wigner-Breight shape with the resonance width determined by parameter γ_b , where γ_b is given by

$$\gamma_b = 2 \frac{(\omega_{def} - \Omega_0)^2}{\omega_u - \Omega_0} e^{-\kappa Na}, \quad (32)$$

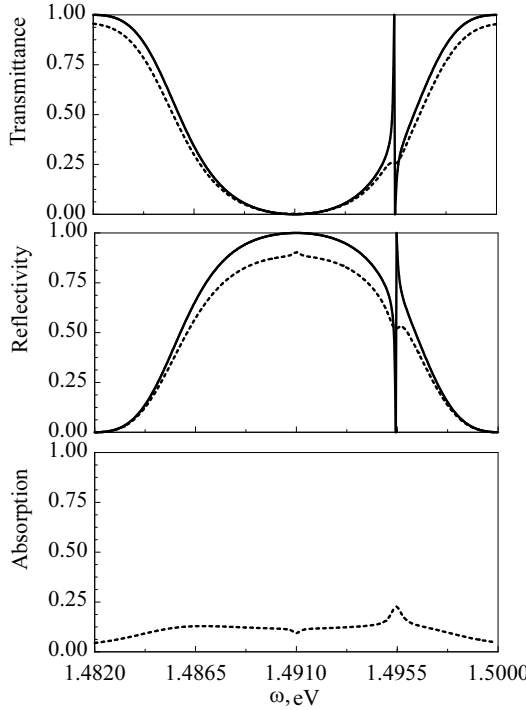


FIG. 5. Transmission, reflection and absorption coefficients for an Ω type defect. The defect is placed in the center of the MQW with 201 quantum wells. The exciton frequency mismatch is equal to $(\Omega_1 - \Omega_0)/\Omega_0 = 1.003$. No absorption - solid lines, and in the presence of homogeneous broadening - dashed lines.

In real systems, enhancement of the transmission coefficient is usually limited by homogeneous broadening of exciton resonances. Two cases are possible when exciton damping is taken into account. It can suppress the resonance transmission, and the presence of the local states can only be observed as an enhancement of absorption at the local frequency. This can be called a weak coupling regime for LPM, when incident radiation is resonantly absorbed by local exciton states. The opposite case, when the resonance transmission persists in the presence of damping, can be called a strong coupling regime. In this case, there is a coherent coupling between the exciton and the electromagnetic field, so that the local states can be suitably called local polaritons. Qualitatively we can assess the effect of absorption on resonances caused by different defects by looking at the widths of the respective spectra. For all types of defects the width of respective resonances exponentially decreases with the length of the system, consequently, in sufficiently long systems all resonances disappear. However, different pre-exponential factors make different defects behave differently at intermediate distances. A simple qualitative estimate would require that the width of the resonances be smaller than the exciton relaxation parameter. Therefore, the resonances where the pre-exponential factor of the width is considerably larger than the relaxation parameter can be observed in the systems of intermediate length. On the one hand the length must be greater the localization length of the respective local mode, and on the other hand, it must be small enough for the width of the resonance to remain larger than the exciton relaxation parameter. The Fano resonance arising in the case of the Ω -defect though, requires special consideration since its vitality is determined by its asymmetry parameter Q rather than the width parameter γ_Ω . Though the latter is determined by a large pre-exponent (of the order of the exciton resonance frequency Ω_0), the former is of the order of the light-exciton coupling constant Γ_0 , which is much smaller. The Fano resonance will likely be washed out as soon as the relaxation rate exceeds this asymmetry parameter Q . In *InGaAs/GaAs* MQW's experimentally studied in Ref. 8, which we use for numerical calculations, the exciton resonance frequency Ω_0 and the exciton-light coupling parameter Γ_0 were respectively equal to $\Omega_0 = 1.491\text{eV}$, and $\Gamma_0 = 27\mu\text{eV}$, while the exciton relaxation parameter was estimated in that paper as $\gamma_{hom} = 0.28\text{meV}$. This particular system is, therefore, not suitable for observation of the Fano resonance in MQW with the Ω -defect. The pre-exponent of the resonance width in the case of the a -defect is of the order of magnitude of the gap width, which is proportional to $\sqrt{\Gamma_0\Omega_0}$. It is considerably larger than γ_{hom} for the *InGaAs/GaAs* MQW's and we expect, therefore, that it can be easily observed in this system. As far as the b -defect is concerned, it gives rise to extremely narrow transmission peaks, which are characterized by a pre-exponential factor of the order of Γ_0 . It, therefore, cannot be observed in *InGaAs/GaAs* MQW's.

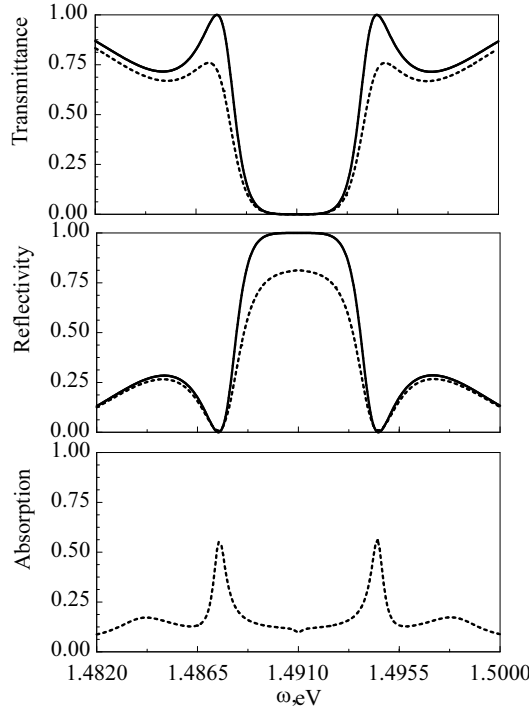


FIG. 6. Transmission, reflection and absorption coefficients for an *a* type defect. The defect is placed in the center of the MQW with 200 quantum wells. The defect strength is $\xi = b/a = 1.5$. No absorption - solid lines, and in the presence of homogeneous broadening - dashed lines.

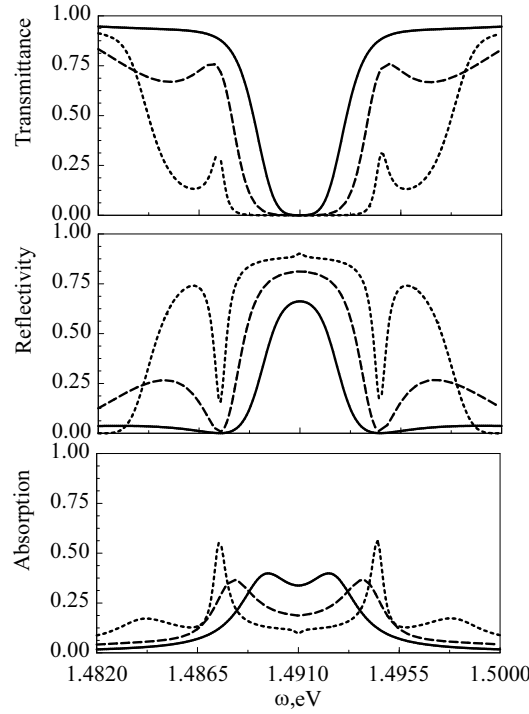


FIG. 7. Transmission, reflection and absorption coefficients for an *a* type defect in the presence of homogeneous broadening for 3 lengths: 100 (solid lines), 200 (dashed lines) and 400 (dotted lines) QWs. The defect is placed in the center of the structure. The defect strength is $\xi = b/a = 1.5$.

We complement the qualitative arguments presented above with numerical calculations of the transmission, reflection, and absorption spectra for different types of defects using parameters of the mentioned *InGaAs/GaAs* system. To account for homogeneous broadening quantitatively we add an imaginary part to the exciton polarizability

$$\beta = \frac{4\Gamma_0\omega}{\omega^2 - \Omega_0^2 + 2i\gamma_{hom}\omega}.$$

Fig. 5 shows transmission and reflection coefficients of the Bragg MQW lattice made of 201 quantum wells with a Ω -defect in the center. One can see that absorption washes out the strong asymmetric pattern of the Fano resonance, but it is interesting that the remains of the resonance are still quite prominent, and can probably be observed in high quality samples. Fig. 6 shows transmission and reflection of the Bragg MQW lattice of 200 quantum wells with an a -defect with $b/a = 1.5$. For this defect one has two symmetric with respect to the center resonances. The peaks are very pronounced in transmission, and the contrast in reflection is very large - about 30%, and can be made even larger if one increases the length of the system. In Fig. 7 we show the evolution of the transmission, reflection and absorption coefficients with the length of the system. For all lengths (100, 200, 400) the defect is situated exactly in the center and its parameters chosen such as to reproduce the most favorable conditions for resonance transition. One can see that peaks in transmission can clearly be seen in the presence of absorption even in the systems as long as $N=400$ and the contrast in reflection reaches 80%. We can conclude, therefore, that in this system the strong coupling between local excitons and local photons can be experimentally realized in *InGaAs/GaAs* MQW's.

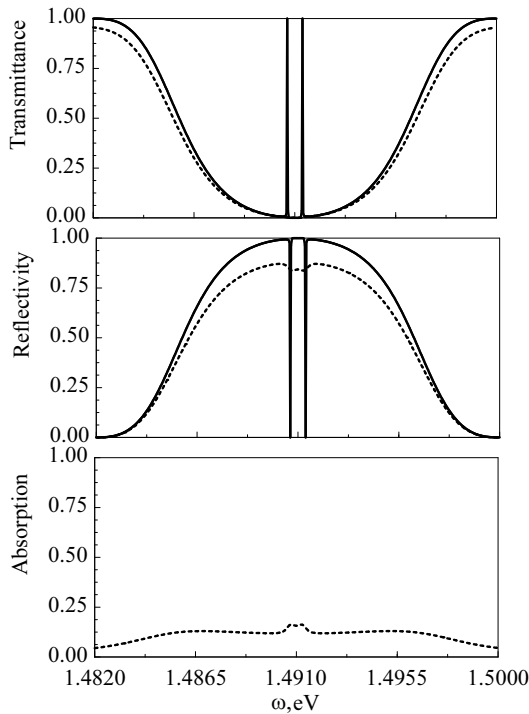


FIG. 8. Transmission, reflection and absorption coefficients for an b type defect. The defect is placed in the center of the MQW with 201 quantum wells. The defect strength $\xi = b/a = 1.5$. No absorption - solid lines, and in the presence of homogeneous broadening - dashed lines.

Fig. 8 shows transmission and reflection for the Bragg MQW lattice 201 QWs long that has the b -defect ($b/a = 1.5$) at the center. It is seen that two very thin peaks in transmission disappear once exciton damping is added. What is interesting, however, is that the resulting absorption of the incident wave is also very weak in the case of Ω - and b -defects. Even though there is some small enhancement of absorption at the resonance frequencies, it is much weaker than absorption peaks in the case of the a -defect. In other words, local polaritons in the regime of strong coupling demonstrate resonance behavior in both transmission and absorption at same time, while in the weak coupling regime there is only a small effect of the local states upon all optical spectra of the system. The explanation for this behavior lies in the spatial distribution of electromagnetic wave intensity throughout the system. In the absence of absorption, the electric field at the resonance frequency decays exponentially away from the defect layer, i.e. there occurs a strong exponential enhancement of the incident field at the defect layer^{16,23}.

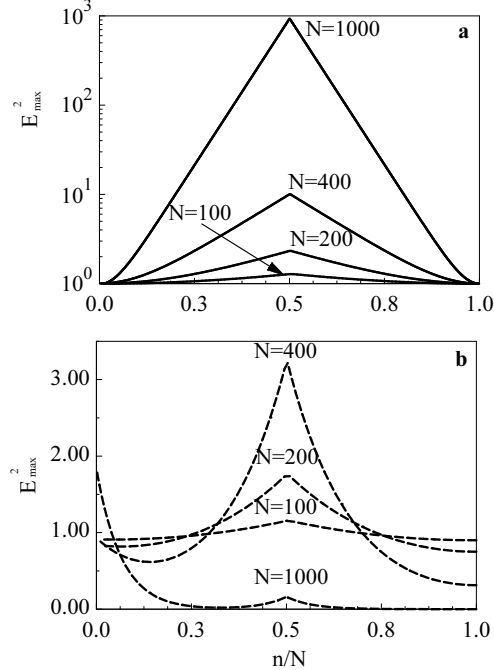


FIG. 9. Distribution of the electric field at the frequency ω_T in the system with an *a*-defect placed exactly in the middle without absorption (a) and with absorption (b). $\xi = b/a = 1.5$. Four curves correspond to different sizes of the system: 100, 200, 400 and 1000 QWs.

Fig. 9a shows the field distribution at ω_T without absorption in the steady state regime. Since without absorption the decay rate is determined by the localization length $l_{loc}(\omega_T)$, the profile is the same for all defects as long as ω_{def} is the same. One can see the exponential increase of the field compared to the amplitude of the incident electromagnetic wave $E_{in} = 1$

$$|E_{max}| = |E_{in}| \cdot e^{(N/2)\kappa a}. \quad (33)$$

Homogeneous broadening suppresses not only the resonance transmission but also the exponential enhancement of the electric field. For the *InGaAs/GaAs* system, which we use for numerical computations this occurs for Ω , Γ and *b*-defects. The intensity of the wave in this case decreases exponentially almost as it would in the absence of defects, and is just slightly larger at the resonance frequency than off-resonance. Therefore, the peaks in absorption in these cases are also only minute. At the same time, Fig. 9b shows that even in the presence of absorption the *a*-defect demonstrates more than a three-fold enhancement of the field at the defect for the system of an optimal length. Fig. 10 shows the evolution of the electric field at the defect as the length of the system grows at ω_T . One can see that the exponential growth of the field in the absence of absorption (dashed curve) changes to a nonmonotonic behavior. For the particular system under consideration, the field reaches its maximum at about $N_m=450$, where we see the crossover from the resonant enhancement regime ($N < N_m$) to the exponential decay ($N > N_m$). Enhancement of the field at the defect explains both transmission and absorption resonances.

IV. CONCLUSION

In the present paper we considered optical properties of multiple quantum well systems where one of the wells is replaced with a structure with different properties, a “defect”. Our interest in such structures is due to additional opportunities to tailor optical properties of quantum heterostructures, which such structures can provide. Our attention was focused upon defect induced effects occurring within a stop-band of the ideal MQW. Though the stop-band does not constitute a complete photonic band-gap specific for 3-d photonic crystals, experiments with cholesteric liquid crystals²⁴ demonstrated that even one-dimensional stop-bands can significantly affect the rate of spontaneous emission and, hence, lasing properties of the system. A possibility to create a local mode within the stop-band can be

used to re-direct (at least partially) spontaneous emission within the frequency interval determined by the width of the local mode. Another important feature of the system under consideration, which distinguishes it from other types of one-dimensional photonic superlattices, is that the local states in our system, if they existed, would be coupled exciton-photon states. This fact provides additional opportunities to control the optical properties of the system affecting its exciton component, for example, by applying external magnetic or electric field. All these opportunities must, of course, be thoroughly investigated in the future, while the present paper is just the first step in this direction, our goal here was to establish an opportunity for such local states to exist in realistic MQW's. As another possible application of the suggested systems, one could use observation of the defect induced changes in optical properties as a way to measure different characteristics of excitons in quantum wells.

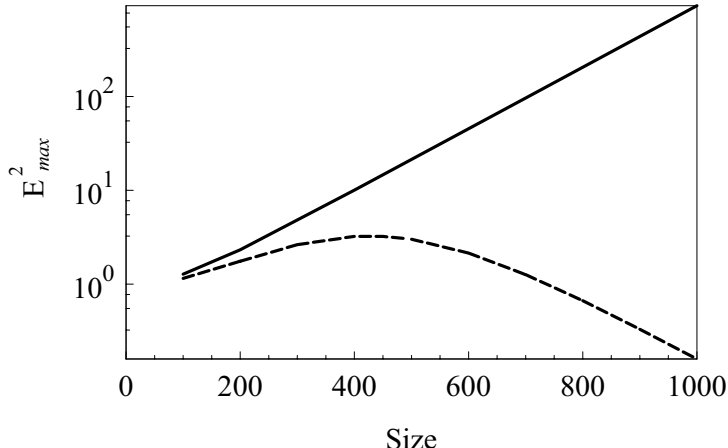


FIG. 10. Dependence of the strength of the electric field at the position of the a -defect (from Fig. 9) at ω_T on the size of the system.

We found that among four different types of defect considered in the paper, only two are of interest. The so called Ω -defect associated with changes in exciton frequency gives rise to a Fano-type transmission resonance. The relation between exciton-photon coupling and exciton homogeneous width in our illustrated system (*InGaAs/GaAsMQW*) smooths out the resonance significantly, and we regard this situation as the case of weak coupling when local polaritons are not actually formed. However, the remnants of the resonance can probably be observed in transmission or reflection. Since Fano resonances have two independent characteristics parameters, which can be extracted from the spectra, these observations can provide a more exact way to measure the exciton resonance frequency, its homogeneous broadening and its reaction to external perturbations. There is also a possibility that in some other systems with greater exciton-photon coupling and/or smaller relaxation, Fano resonances can exist in the strong-coupling regime. In this case, MQW's with the Ω -type defect could provide a system with a narrow transmission/absorption, and hence, emission line, which could be interesting for different applications.

Even more interesting, however, was the defect caused by a change in an interwell spacing between two identical wells (a -defect). This defect is characterized by the parameter $\xi = b/a$, where a is the period of the structure, and b is the changed spacing, and gives rise to two strong transmission and absorption resonances within the polariton band-gap of readily available *InGaAs/GaAs* multiple quantum wells. Our calculations provide explicit details on the characteristics of the system (the defect interwell spacing, the number of wells, etc.) which would produce the optimal results. Formally, the system with an a -defect looks like a regular cavity with two mirrors. There is, however, a significant difference between the system under consideration and regular distributed Bragg reflectors. Unlike regular cavities, which are used as a container for optically active elements, in our system the mirrors themselves are optically active. This fact affects all the properties of the system: frequencies of the "cavity" modes, spatial distribution of the field, and possible applications. Therefore, we regard MQW's with the a -defect as a new type of quantum heterostructure. This defect can be implemented experimentally by means of a simple change in the thickness of one of the barrier layers in the process of growth. One can notice, however, that the parameter ξ is actually determined by optical widths of the respective layers, rather than by their geometrical characteristics. Therefore, it is possible to implement this defect by means of replacing one of the barrier layers with a material with different dielectric (or magnetic) permeabilities. This provides even greater opportunities in manipulating optical properties of the system. Exploration of these opportunities, however, has to be left to future studies.

ACKNOWLEDGMENTS

We are indebted to S. Schwarz for reading and commenting on the manuscript. This work was partially supported by NATO Linkage Grant N974573, CUNY Collaborative Grant, and PSC-CUNY Research Award.

- ¹ D. S. Citrin, Solid State Commun. **89**, 139 (1994).
- ² E. L. Ivchenko, A. I. Nesvizhskii, and S. Jorda, Phys. Solid State **36**, 1156 (1994).
- ³ L. C. Andreani, Phys. Lett. A **192**, 99 (1994); Phys. Status Solidi B **188**, 29 (1995).
- ⁴ G. Björk, S. Pau, J.M. Jakobson, H. Cao, and Y. Yamamoto, Phys. Rev. B **52**, 17310 (1995).
- ⁵ M. Hübner, J. Kuhl, T. Stroucken, A. Knorr, S. W. Koch, R. Hey, K. Ploog, Phys. Rev. Lett. **76**, 4199 (1996).
- ⁶ T. Stroucken, A. Knorr, P. Thomas, and S. W. Koch, Phys. Rev. B **53**, 2026 (1996).
- ⁷ M. P. Vladimirova, E. L. Ivchenko, and A. V. Kavokin, Semiconductors **32**, 90 (1998).
- ⁸ M. Hübner, J. P. Prineas, C. Ell, P. Brick, E. S. Lee, G. Khitrova, H. M. Gibbs, S. W. Koch, Phys. Rev. Lett. **83**, 2841 (1999).
- ⁹ L. I. Deych, and A. A. Lisyansky, Phys. Rev. B **60**, 4242 (2000).
- ¹⁰ I.M. Lifshitz and A.M. Kosevich, in: *Lattice Dynamics* (Benjamin, New York, 1969), p. 53.
- ¹¹ D. S. Citrin, Appl. Phys. Lett. **66**, 994(1995).
- ¹² A. Dereux, J.-P. Vigneron, P. Lambin, and A. Lucas, Phys. Rev. B **38**, 5438 (1988).
- ¹³ M. L. H. Lahlaouti, A. Akjouj, B. Djafari-Rouhani, and L. Dobrzynski, Phys. Rev. B **61**, 2059 (2000).
- ¹⁴ L.C. Andreani, “Optical Transitions, Excitons, and Polaritons in Bulk and Low-Dimensional Semiconductor Structures,” in: *Confined Electrons and Photons* (edited by E. Burstein and C. Weisbuch, Plenum, New York, 1995).
- ¹⁵ L. I. Deych and A. A. Lisyansky, Phys. Lett. A **243**, 156 (1998); L. I. Deych, A. Yamilov, and A. A. Lisyansky, Europhys. Lett. **46**, 524 (1999).
- ¹⁶ L. I. Deych, A. Yamilov, and A. A. Lisyansky, Phys. Rev. B **59**, 11339 (1999).
- ¹⁷ A. Yamilov, L. I. Deych, and A. A. Lisyansky, J. Opt. Soc. Amer. B **17**, 1498 (2000).
- ¹⁸ I. H. Deutsch, R. J. C. Spreeuw, S. L. Rolston, and W. D. Phillips, Phys. Rev. A **52**, 1394 (1995).
- ¹⁹ L. V. Keldysh, Superlattices and Microstructure **4**, 637 (1988).
- ²⁰ E. L. Ivchenko, Phys. Solid State **33**, 1344 (1991).
- ²¹ U. Fano, Phys. Rev. **124**, 1866 (1961).
- ²² G. Breit and E. Wigner, Phys. Rev. **49**, 519 (1936).
- ²³ M. Ya. Azbel, Solid State Comm. **45**, 527 (1983).
- ²⁴ V. I. Kopp, B. Fan, H. K. M. Vithana, and A. Z. Genack, Optics Lett. **23**, 1707 (1998).